Conf-780609--12

1/ 7-17-78

COMPARISON OF ICEPEL PREDICTIONS WITH SINGLE ELBOW FLEXIBLE PIPING SYSTEM EXPERIMENT

by

M. T. A-Moneim and Y. W. Chang

MASTER

Prepared for

ASME/CSME Pressure Vessel and Piping Conference
Montreal, Canada
June 1978

U of C-AUA-USDOE

ARGONNE NATIONAL LABORATORY, ARGONNE, ILLINOIS

Operated under Contract W-31-109-Eng-38 for the
U. S. DEPARTMENT OF ENERGY

COMPARISON OF ICEPEL PREDICTIONS
WITH SINGLE ELBOW FLEXIBLE
PIPING SYSTEM EXPERIMENT

by

M. T. A-Moneim and Y. W. Chang

Argonne National Laboratory

ABSTRACT

The ICEPEL Code for coupled hydrodynamic-structural response analysis of piping systems is used to analyze an experiment on the response of flexible piping systems to internal pressure pulses. The piping system consisted of two flexible Nickel-200 pipes connected in series through a 90° thick-walled stainless steel elbow. A tailored pressure pulse generated by a calibrated pulse gun is stabilized in a long thick-walled stainless steel pipe leading to the flexible piping system which ended with a heavy blind flange. The analytical results of pressure and circumferential strain histories are discusses and compared against the experimental data obtained by Stanford Research Institute.

1. INTRODUCTION

Experimental investigations in physical sciences have long been used to help understand the physical phenomena involved. The insights gained from these investigations can also help analyze the phenomena closely. Recently, the advances in computer technology have made possible the analysis of complex phenomena by computer codes, but the process usually involves some simplifications and assumptions. Therefore, experimental verification of such codes is necessary to increase the confidence in their performances. Well designed experiments can also help modify and simplify such codes for better efficiency.

ICEPEL is a transient two-dimensional code for coupled hydrodynamic-structural response analysis of piping systems under the effect of simultaneous pressure pulses [1]. The code utilizes an implicit continuous-fluid Eulerian finite difference method in describing the hydrodynamics. For the structural part the walls are treated as thin axisymmetric shells in which the analysis considers both the membrane and bending strengths of the material. However, only the hoop stress mode of deformation resulting from internal pressurization is considered.

A convected coordinate finite element method for large displacement but small strains, elastic-plastic structural dynamics is utilized [2]. The walls are replaced by straight elements connected together thorough nodes. Each element is associated with a set of convected coordinates that rotate but do not deform with the element. Both strains and nodal forces are assumed linearly

---

1. A-Moneim, M. T., "Coupled Hydrodynamic-Structural Response Analysis of Piping Systems", ANL Report to be published.

2. Belytchko, T. and Hseih, B. J., "Nonlinear Transient Finite Element Analysis With Convected Coordinates", Int. Journal of Numerical Methods in Engineering, 7,255-271 (1973).

related, respectively, to the displacement and stresses relative to the nodal coordinates. Important nonlinearities from large rotations are entirely accounted for by the transformation between the convective and global coordinates. Nonlinearities in material behavior are, however, considered as a multilinear stress-strain relationship.

The structural and hydrodynamic calculations are coupled together in each time step in such a way that the hydrodynamics supplies the structure with a pressure loading and gets back a moving boundary condition to match. The fluid is allowed to slide freely along the wall but move with the wall in a direction normal to it.

Several hydrodynamic models for the different piping components are available in the code (an elbow, generalized piping component, a tee, and a surge tank). They are hydrodynamically coupled together so that a general piping system can be represented.

An experimental program for the verification of the different models and the coupling techniques in the ICEPEL code was undertaken. The first phase of it consists of five simple experiments designed at Argonne National Laboratory and performed by the Stanford Research Institute. Two straight flexible pipe tests, FP-SP-101 and FP-SP-102, and three single elbow loop tests, FP-E-101, FP-E-102, and FP-E-103, were performed [3]. All tests have been analyzed by the ICEPEL code and the results were compared against the experimental results. In this paper, the analysis and the comparison between the analytical and experimental results of the single elbow loop test FP-E-103 is reported.

---

3. Romander, C. M. and Cagliostro, D. J., "Experiments on the Response of Flexible Piping Systems to Internal Pressure Pulses", SRI Fourth Interim Report, April 1976.

2. DESCRIPTION OF EXPERIMENT

A schematic of the experimental layout and the instrumentation locations of the single elbow loop test is shown in Fig. 1. A pulse gun is directly flanged to a thick-walled stainless steel pipe of 8.26 cm (3.25 in) outside diameter, 0.48 cm (0.188 in) wall thickness, and 304.8 cm (10 ft) length. The thick-walled stainless steel pipe is directly flanged to a flexible Nickle-200 pipe which is 152.4 cm (5 ft) long and has an outside diameter of 7.62 cm (3 in), and a wall thickness of 0.165 cm (0.065 in). This flexible pipe is connected in series to an identical pipe through a 90° thick-walled stainless steel elbow of 11.43 cm (4.5 in) radius of curvature. Two short transition pieces are welded to both ends of the elbow to gradually change the inside diameter from that of the elbow (7.06 cm, 2.78 in) to a diameter of 7.24 cm (2.85 in) which itself is less than that of the connected flexible pipes of 7.29 cm (2.87 in). Measurements of the elbow cross-section at the different locations showed a slighlty egg-shaped cross-section with the inside diameter varying from one end to the other.

The second flexible pipe ended with a heavy blind flange in test E-102 and E-103. All flanges were well sealed and were connected to heavy brackets which were anchored to the ground to limit both the lateral and longitudinal motions of the flanges, which is a requirement of the ICEPEL code. The system was full of water at the moment of charge detonation in the pulse gun.

A total of eighteen pressure transducers, shown by P1 through P18, were used to monitor the pressure pulse propagation along the system. Up to three pressure transducers were mounted at the same axial location before and after the elbow to check the effects of the elbow on the axisymmetry of the flow inside the pipes. Also, three pressure transducers, P11 through P13, were mounted at the midsection of the elbow to record the radial pressure distribution inside the elbow.

Twenty strain gages, shown by SG_1 through SG_{20}, were used at four axial locations in the first flexible pipe to monitor its response to the traveling pressure pulses. Strain gages were distributed in groups of five at 60° intervals at each axial location to check the uniformity of strains around the circumference of the pipe. The second flexible pipe was not instrumented with strain gages.

3. ICEPEL ANALYTICAL MODEL

Since only pressure histories of the form P(t) can be used as an input to an ICEPEL model of a piping system, the pressure history as recorded by gage P1 is used an an input pulse to the pipe system downstream from it. Thus, the ICEPEL model of the pipe system considers only 228.6 cm (90 in) of the thick-walled stainless steel pipe directly connected to the Nickel-200 flexible pipes with a rigid elbow in between. However, the elbow in the model has the same inside diameter as the Nickel-200 pipes.

All pipes are divided into equal finite difference zones of 1.82 cm radial zone size and 2.54 cm (1 in) axial zone size. The elbow itself is divided into four radial zones and five tangential zones.

The walls of the thick-walled stainless steel pipe is considered in the model as made of Nickel-200, the same material as the flexible test pipe, but with an 1 cm thick wall to limit its response to elastic response. The walls of the flexible pipes are 0.165 cm thick.

The heavy blind flange at the end of the second flexible pipe and the rigid elbow are represented by fixed shell nodes, i.e. neither translation or rotation is permitted at such nodes.

4. PIPE MATERIAL PROPERTIES

Stress-strain properties of Nickel-200 were measured by SRI on a specimen cut from a scrap section of the Nickel-200 pipes. The specimen was flattened then annealed in exactly the same way the test pipes were annealed.

Stress-strain properties were measured at two strain rates to examine if Nickel-200 is strain rate dependent or not. The results are shown in Fig. 2 at two different strain rates. No significant effect was found for a three-order-of-magnitude increase in strain rate. Hence, it was concluded that Nickel-200 is nearly free of strain rate effects.

Since the actual strain rate in the pipe tests is about three-order-of-magnitudes higher than the highest strain rate of the material property tests, the stress-strain properties at the higher strain rate is considered to approximate those of the test pipes.

In the ICEPEL code, stress-strain relationships are approximated by a multilinear stress-strain curve. Attempts to closely approximate such a behavior with a bilinear relationship usually end with a higher yield stress than the true yield stress of the material in order to best approximate the plastic part of the curve. Such an approximation is acceptable if the strains are known to be well in the plastic region.

However, in a piping system, the magnitude of the pressure peaks transmitted beyond the region of plastic wall deformation depends on the yield pressure of the pipe. A higher yield stress for the pipe wall material permits transmission of higher pressure peaks.

Consequently, the pressure pulses that result from the interaction of the transmitted pressure pulse with piping components or with flow-area-changes in the system and the plastic wall deformation resulting from them are bound to be over-estimated only as a result of having a higher yeild stress for the wall material.

This type of result was observed on a preliminary model of the straight pipe tests in which a bilinear stress-strain relationship was used. Higher pressure peaks were transmitted beyond the region of plastic-wall deformation. This resulted in higher pressures reflecting from the blind flange and higher strains in this vicinity. Reducing the yield stress in a bilinear stress-strain relationship reduced the transmitted pressure peaks and hence reduced the strain at the right end of the pipe.

Therefore, a quadrilinear stress-strain relationship is used to approximate the stress-strain properties at the higher strain rate. Such relation are shown in Fig. 2 by the circles and are listed in Table 1.

Table 1

Stress-strain Values of Nickel-200

used in Code Calculations

Stress, MPa	Strain, cm/cm
76	0.000393
95	0.00127
118.6	0.0058
384	0.1

5. COMPARISON OF ICEPEL RESULTS WITH EXPERIMENTAL DATA

The input pressure pulse for the analytical model is shown in Fig. 3 as recorded by gage P1 in test FP-E-103. Figures 4 and 5 show the comparison between the analytical and experimental pressure histories at locations P2 and P3 inside the thick-walled pipe. As can be seen, a very good agreement in so far as the pulse shape and arrival time is obtained. However, the analytical pressure peak magnitude are lower than the experimental peaks particularly at gage P3. One reason for this is the inherited feature of the implicit finite difference methods in smearing off sharp peaks as those of location P2 and P3. The use of smaller hydrodynamic time step in the calculation was found to improve the resolution of sharp pressure peaks. It should be noted here that the experimental pressure history at gage P3 shows much higher pressure peak than that at gages P1 and P2 upstream from P3. That explains why the difference between the analytical and experimental pressure peaks is higher at gage P3 than at gage P2.

Indicated also in the figures is the effects of the right to left moving rarefaction wave reflecting back from the flexible pipe, causing cavitation to occur at gage P2 which is indicated by the bottoming of the experimental pressures at about 2.5 ms. The calculations agreed in predicting the occurance of cavitation at this location by the zero pressure which is the cut off pressure in the ICEPEL code. The effect of the same reflected rarefaction wave on the pressure history at gage P3 is the fast unloading of the incident pulse.

The last pressure peak obtained in the analysis is a result of the reflected pressure pulse from the closed rigid end of the second flexible pipe. No pressure records were reported at locations P2 and P3 beyond 3 ms.

In Fig. 6 and 7, the comparison between the analytical and experimental pressure histories at the beginning of the first flexible pipe at gages P4 and P5 is shown. A very good agreement in all aspects of the incident pressure pulse is obtained. However, the analysis is showing slightly higher pressures than the experimental pressure in the tail portion of the incident pulse at location P4 which is the closest position to the flange between the thick-walled pipe and the flexible pipe. This flange which can be responsible for the noise in the experimental data is not modeled in the analysis.

The figures also indicate the effect of plastic pipe wall deformation on the traveling pulse. The pressure peaks are rapidly attenuated to about 6 MPa in only 3.81 cm (1.5 in) and further reduced to about 5 MPa in 15.24 cm (6 in). The dispersion of the pulse is also indicated in the broadening of the pressure pulse compared to the pulses in the thick-walled pipe.

The reflected pressure pulse from the blind flange at the end of the second flexible pipe indicated by the last pressure peak, is shown to be slightly higher analytically than experimentally. As will be seen later, this is consistent at all locations. The reason for this is believed to be the conservative nature of modeling the blind flange as a rigid dead end. Experimentally, although the flanges were anchored to the ground to limit their motion, some of the incident pulse energy is expanded in axially expanding the pipe as the pulse hits the flange.

As the pulse travels along the first flexible pipe plastic pipe wall deformation further attenuates the pressure peaks down to a value of about 4 MPa which is slightly higher than the yield pressure of the pipe (3.5 MPa) because of the inertia of the pipe wall. This is seen in Figs. 8 through 10 which show the comparison between the analytical and experimental pressure histories at gages P6, P7 and P8-P10 of the first flexible pipe. Again the agreement in all aspects of the pressure pulse is demonstrated. Comparatively, however, the agreement at gage P6 of Fig. 8 is not as good as those at the other gages. The analysis is showing higher pressures than in the experiment. Examination of the experimental pressure histories upstream and downstream from gage P6 indicates that gage P6 may have been in error recording lower pressures.

Figure 10 indicates that the experimental records of gages P8-P10 showed no variation of pressure around the circumference of the pipe. Thus confirming the axisymmetry of the flow in the pipe upstream from the elbow, an assumption used in the ICEPEL hydrodynamic coupling of the pipe and elbow models.

Downstream from the elbow, at gages P14-P16 and P17-P18, the comparison between the analytical and experimental pressure histories is shown in Figs. 11 and 12. Again, the experimental records there confirms the axisymmetry of the flow in the pipe downstream from the elbow showing no effect of the elbow. At both locations the analysis has consistently overestimated the pressures. The reason is that experimentally the elbow attenuated the pressure peaks by as much as 18%, while the analysis did not show that much attenuation.

In fact, the analysis showed no drop in peak pressures in its absolute sense. However, a careful investigation of the analytical pressure histories before and after the elbow reveals some kind of loss inside the elbow. Fig. 10 shows that the pressure histories before the elbow to have an almost flat pressure peak of about 4 MPa that lasted for about 0.75 msec. Fig. 11 shows that the pressure history after the elbow rose at the same rate as that location P8-P10, before the elbow, until a pressure of about 3.5 MPa was reached; then the pressure continued to increase but at a reduced rate until it reached a peak of 4 MPa, which lasted only for a brief time compared to the peak time before the elbow.

A source of the experimental pressure peaks attenuation along the elbow is the geometry of the elbow which had a slight ovality in section. Also, the elbow had a nominal inside diameter of 7.06 cm and was connected to short transition pieces that increased the diameter to 7.24 cm which itself is less than the inside diameter (7.29 cm) of the connected pipes. This geometry cannot be included in the analytical model.

Inside the elbow, the analysis showed that the pressures near the outer walls of the elbow is higher than the pressures near the inner walls, whereas the experimental data showed no special trend, i.e., there was no significant difference in the pressure inside the elbow. Theoretically, one expects higher pressures near the outer walls of the elbow than near the inner walls because of the curvature and centrifurgal effects. Among all the three elbow tests, only the elastic test FP-EP-102 showed higher pressures near the outer walls than near the inner walls of the elbow.

The analytical and experimental strain histories in the first flexible pipe are compared in Figs. 13 through 16. At each axial location the analytical strain histories as predicted by the ICEPEL code are within the rather wide scatter of the experimental strain measurements. Generally, the analytical and experimental strain histories agreed in shape and in peak-strain arrival time. Both the analysis and the experiment indicated the arrival of the reflected pressure pulse from the blind flange at the end of the second flexible pipe.

The small negative strains at the last axial location of the first flexible pipe was measured experimentally and also predicted analytically. This can be attributed to the precursor effects which result from the difference of wave speeds in the pipe wall and in the fluid. The wave propagates slower in the fluid.

The experimental variation in strains around the circumference of the pipe was first attributed to nonuniformity of the pipe wall thickness. The pipe was a commercial off the shelf pipe in which the wall thickness was found to vary within ±5% around the circumference. But, because of the large variations in strains and because of the inconsistency between the strains and wall thickness (i.e. highest strains did not always occur at the smallest thickness location), one is led to believe that variations in wall thickness cannot be totally responsible for the recorded strain variations. Such variation in thickness around the circumference of the pipe cannot be modeled in the ICEPEL code which treats the walls as axisymmetric thin shell.

Another source of variation of strains around the circumference is bending of the pipe which can result from imperfections in the commercial pipe used.

Examination of the records of the different strain gages for test FP-E-103 shows that the highest strains at the first two axial locations were measured by gages SG_1 and SG_2 for the first axial location and by gages SG_6 and SG_7 for the second axial location. Whereas at the other end of the pipe the highest strains were measured by gages SG_{14} and SG_{15} at the third axial location and by gages SG_{19} and SG_{20} at the fourth axial location. Referring to the location of these gages in Fig. 1, this may indicate the second bending mode for the first flexible pipe.

Another noteworthy remark is that the analysis predicts higher strains near the elbow (SG_{16} - SG_{20}, Fig. 16) than further away from the elbow (SG_{11} - SG_{15}, Fig. 15). This indicates a pressure pulse reflecting back from the rigid elbow to the first flexible pipe. However, because of insufficient strain measurements in the vicinity of the elbow and because of the variations in experimental strain at the same axial location this conclusion cannot be drawn.

6. SUMMARY AND CONCLUSIONS

For the physical phenomena of pressure pulse propagation along pipe systems, it has been demonstrated both experimentally and analytically that although plastic pipe wall deformation rapidly attenuate high pressure peaks to magnitudes slightly higher than the yield pressure of the pipe, the subsequent interaction of the transmitted pressure pulses with the different piping components and with other traveling pulses can produce: (a) pressure pulses of bigger magnitude that cause more plastic deformation to occur elsewhere, or (b) a rarefaction pressure wave that may cause cavitation to occur. The more complex the pipe system is the harder it is to follow the pressure pulses and to predict the severity and location of the critical regions in the system.

It has also been demonstrated that the ICEPEL predictions have generally agreed with the experimental measurements of pressure and strain histories. All aspects of the time histories were in very good agreement. The elbow, however, appear to need further analytical as well as experimental investigations to resolve the question of radial pressure distribution inside the elbow and the pressure peak attenuation along the elbow.

In the course of analyzing and comparing the analytical and experimental results of the other two single elbow loop tests FP-E-101 and FP-E-102 [4], it was found that there is an analytical peak pressure drop of about 7% in test FP-E-101 which differed from test FP-E-103 only in having the end of the second flexible pipe open. Also, as mentioned before, the experimental pressure measurements inside the elbow showed higher pressures near the outer walls than near the inner walls, in agreement with the analysis.

Therefore, it is to be recommended here that a precision elbow test be performed to help resolve these inconsistencies. In such a test more strain gages should be axially mounted in the vicinity of the elbow in both pipes to monitor any pressure pulse reflections from the rigid elbow. Reflections from the elbow can be seen in strain measurements more so than in pressure measurements.

The experimental strain varations around the circumference of the pipe is not totally due to the variation in pipe wall thickness. The same mathematical model when used once with the pipe wall thickness equals the smallest measured thickness and once with the largest measured thickness showed only about 15% difference in the strain at the same axial location of the pipe. Bending of the pipe resulting from pipe imperfections is another source of strain variations around the pipe circumference. This signals the importance of including the flexural stresses of the pipe wall to the hoop stresses in the

---

4. A-Moneim, M. T., "ICEPEL Analysis of and Comparison with Simple Elastic-Plastic Piping Experiments", ANL Report to be published.

analysis. Experimentally a precision pipe experiment can eliminate the wall thickness variation.

ACKNOWLEDGMENT

This work was performed in the Engineering Mechanic Section of the Reactor Analysis and Safety Division of Argonne National Laboratory under the auspices of the U.S. Department of Energy.

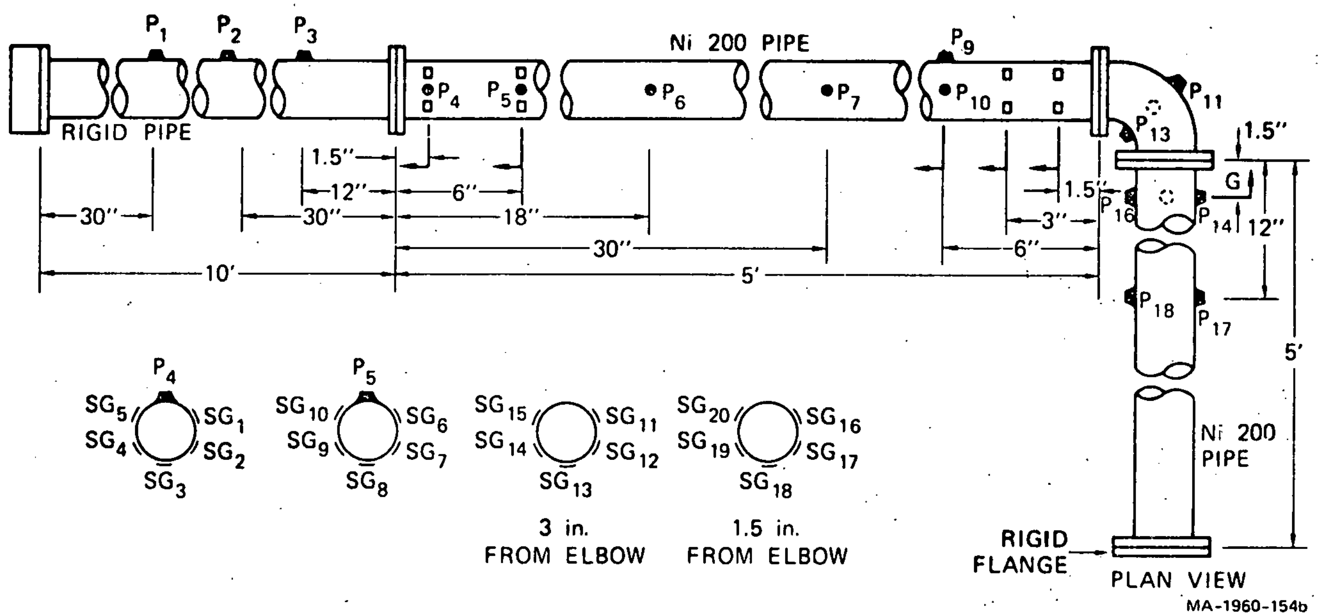

Fig. 1. Layout of the SRI Pipe-Elbow Experiment E-103.

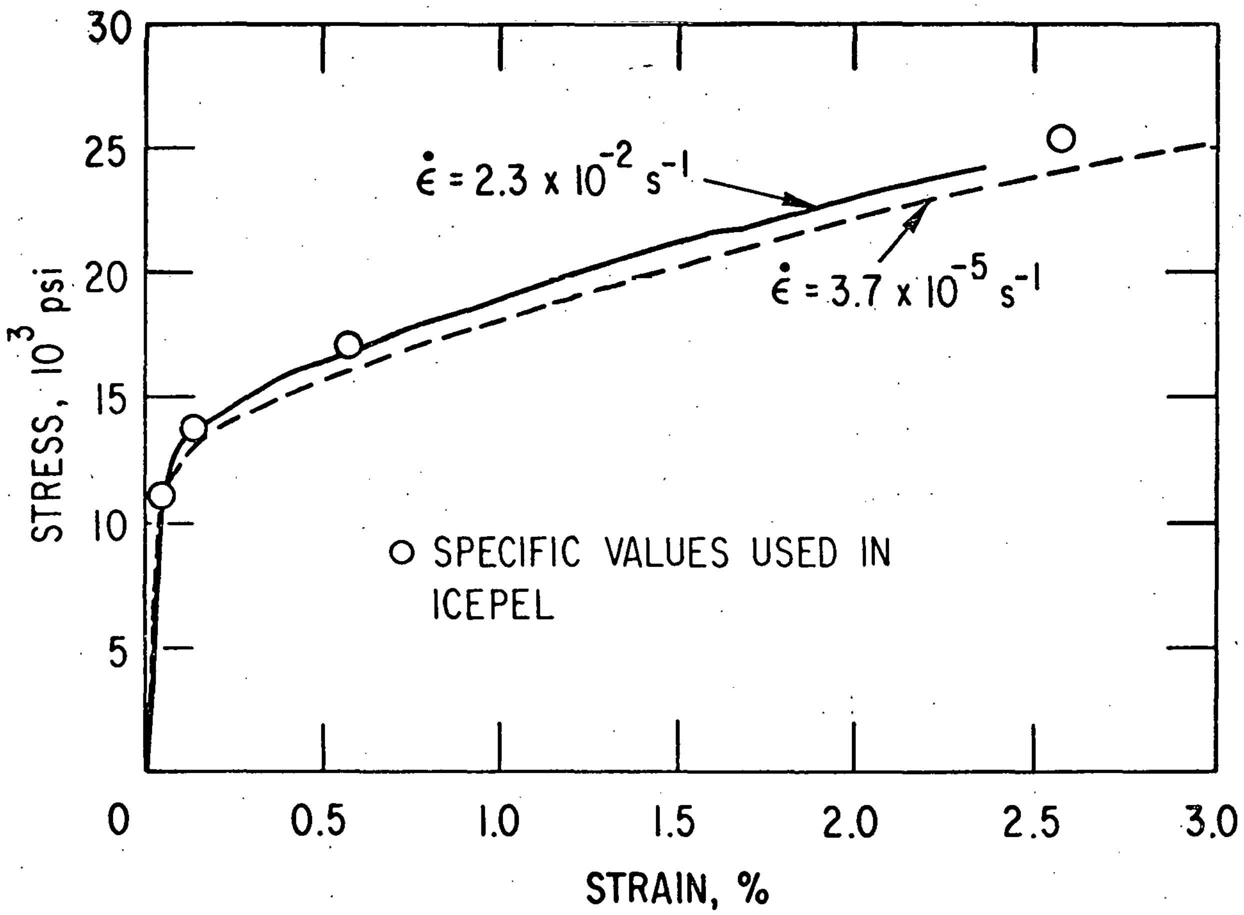

Fig. 2. Stress-Strain Relationship for Nickel-200.

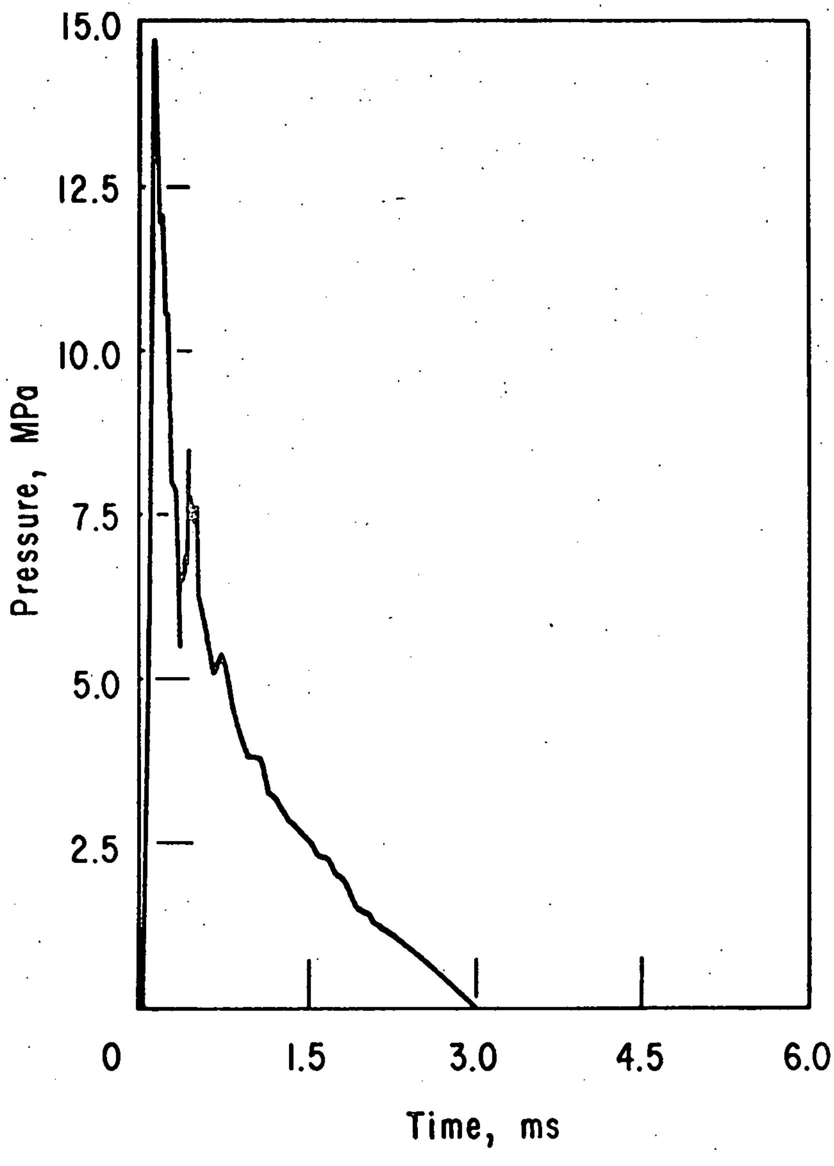

Fig. 3. Input Pressure Pulse (Gage P1, SRI).

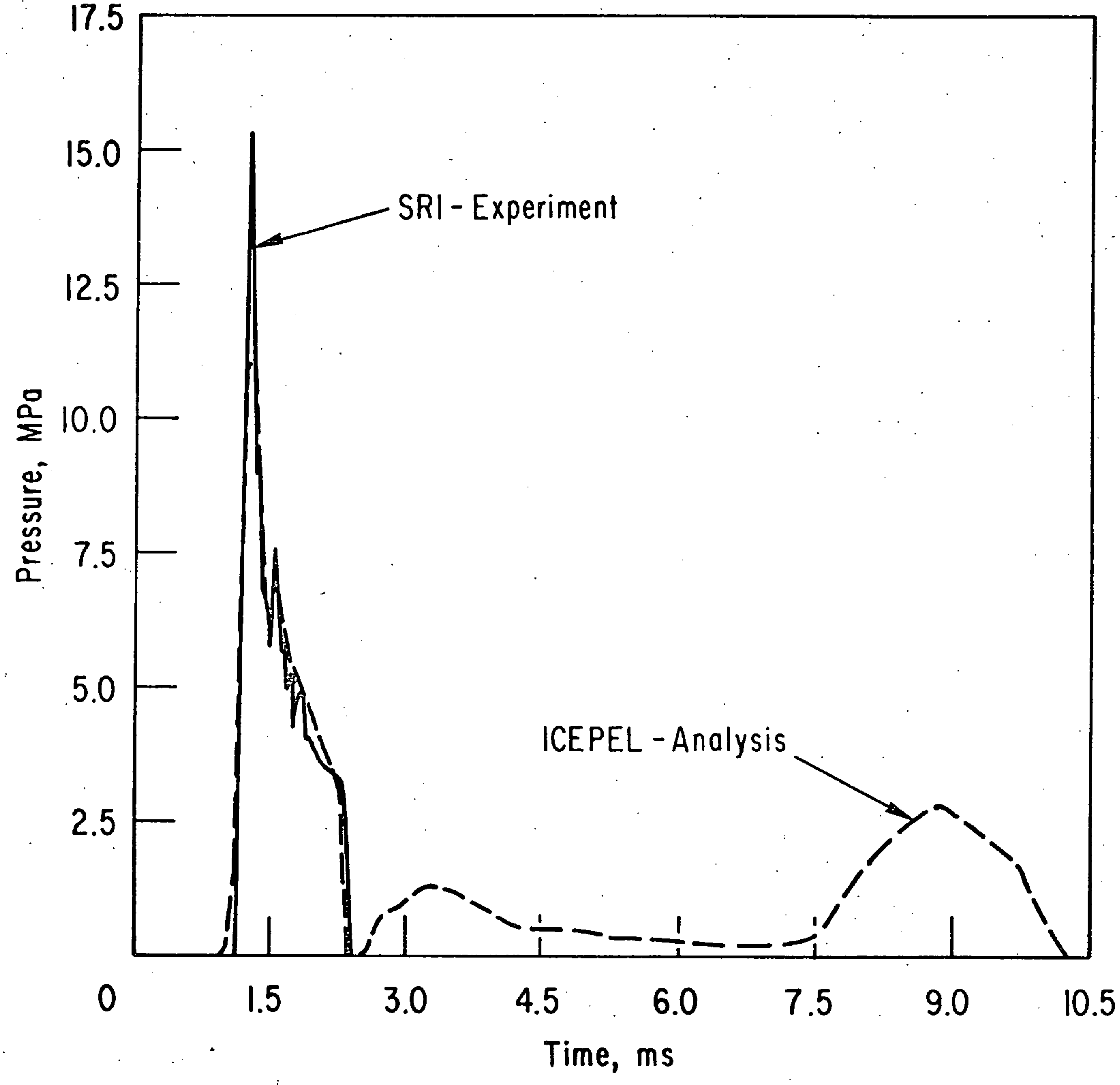

Fig. 4. Analytical and Experimental Pressure Histories at Location P2 in the Rigid Pipe.

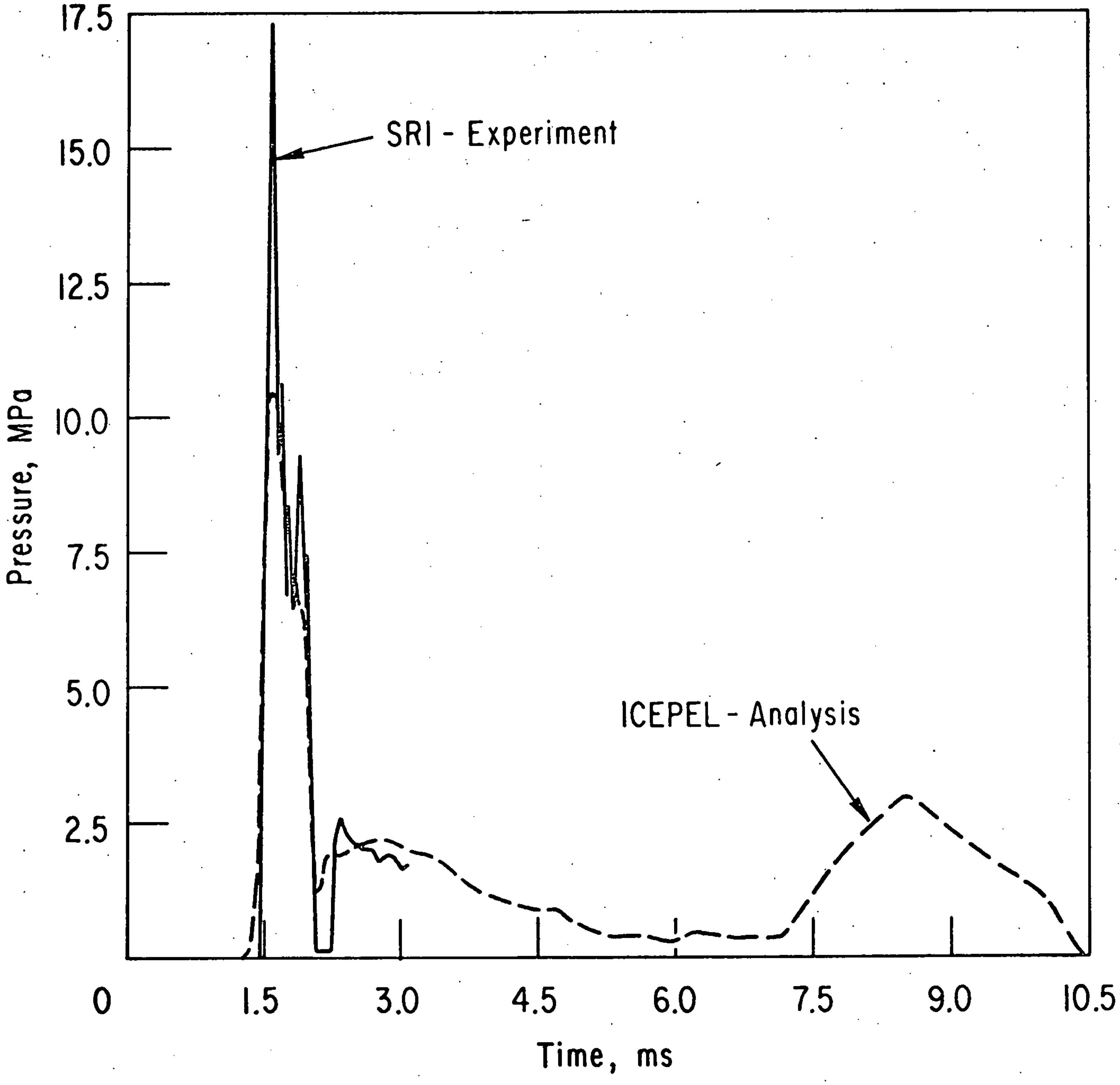

Fig. 5. Analytical and Experimental Pressure Histories at Location P3 in the Rigid Pipe.

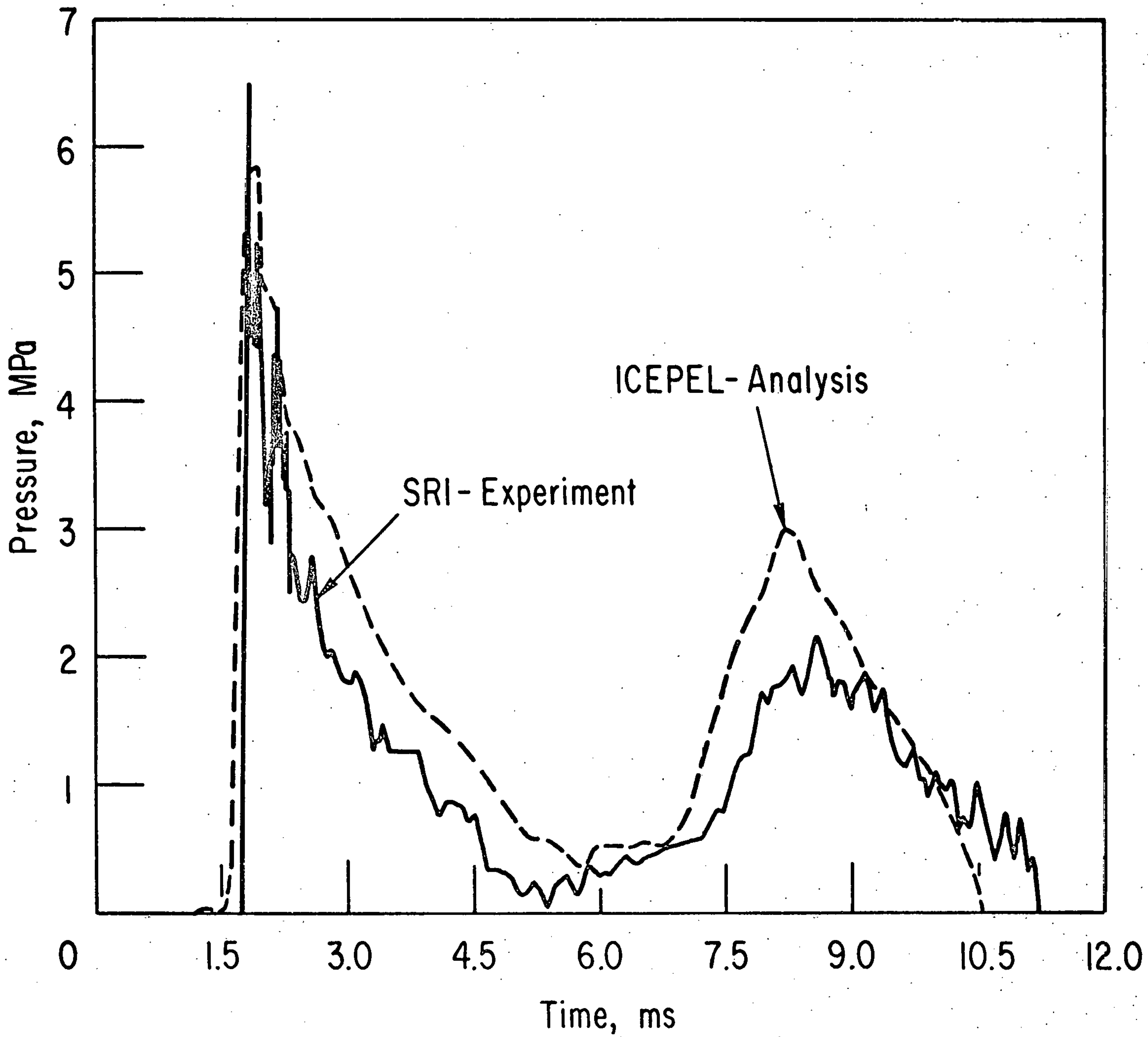

Fig. 6. Analytical and Experimental Pressure Histories at Location P4 Inside the First Flexible Pipe.

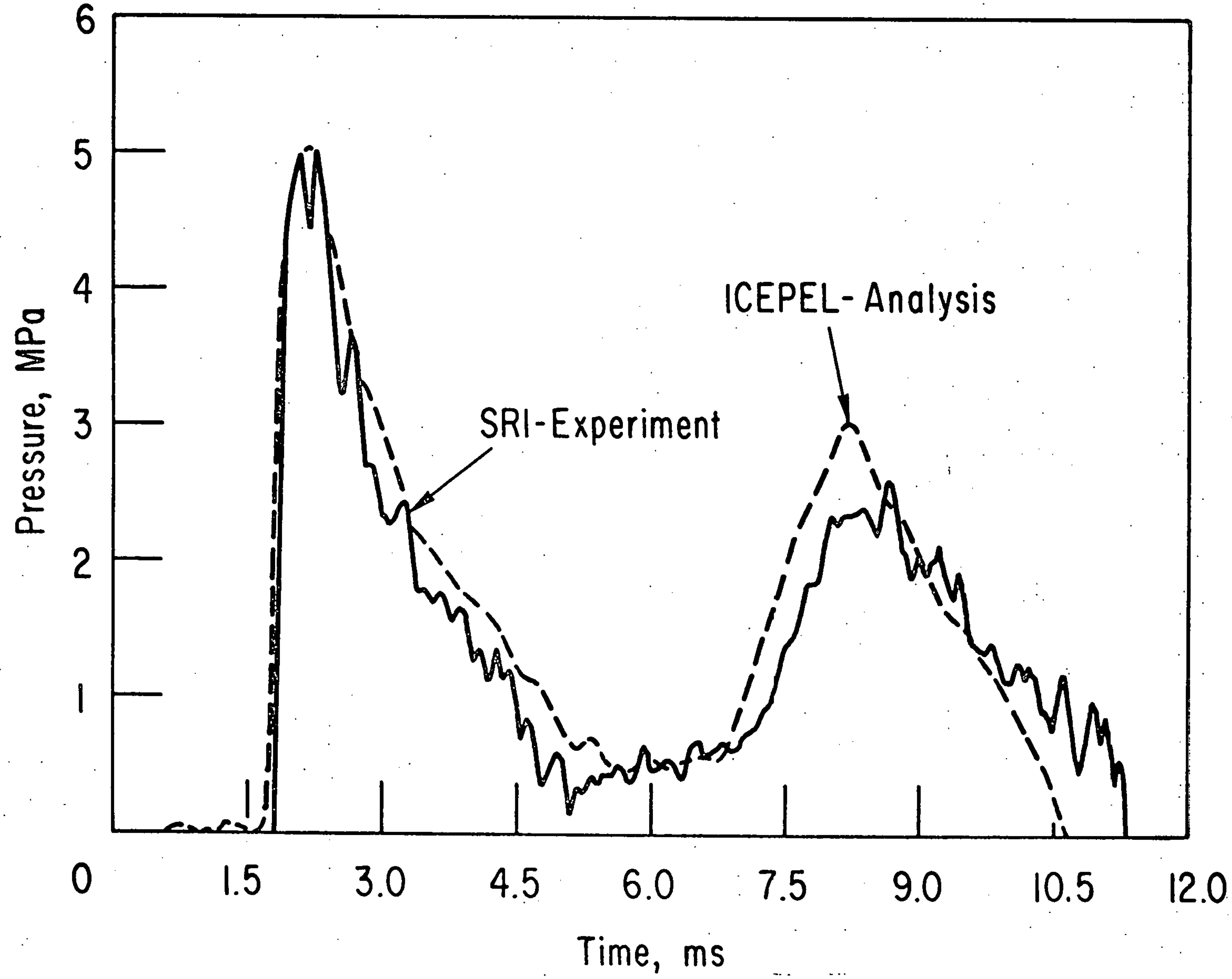

Fig. 7. Analytical and Experimental Pressure Histories at Location P5 in the First Flexible Pipe.

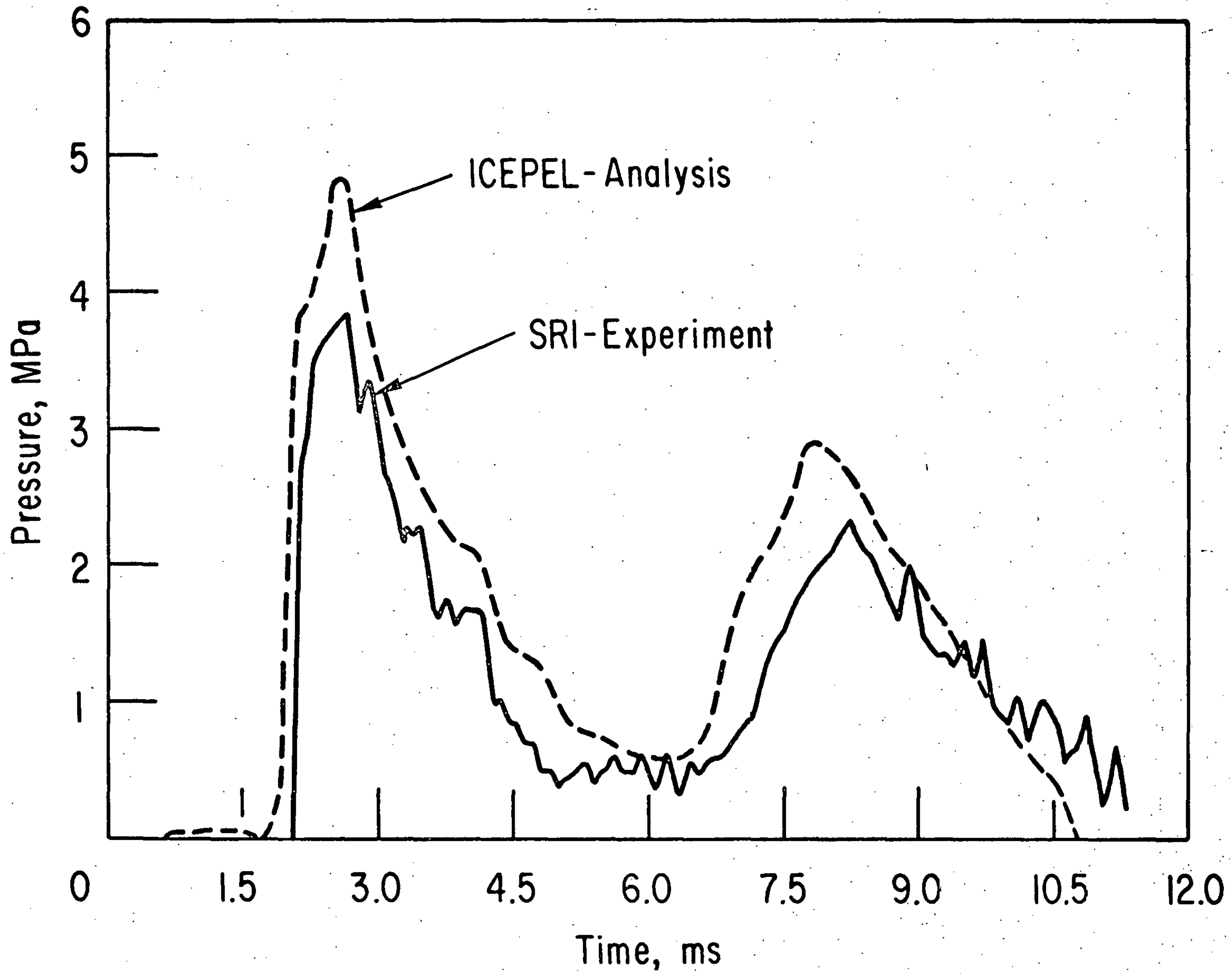

Fig. 8. Analytical and Experimental Pressure Histories at Location P6 of the First Flexible Pipe.

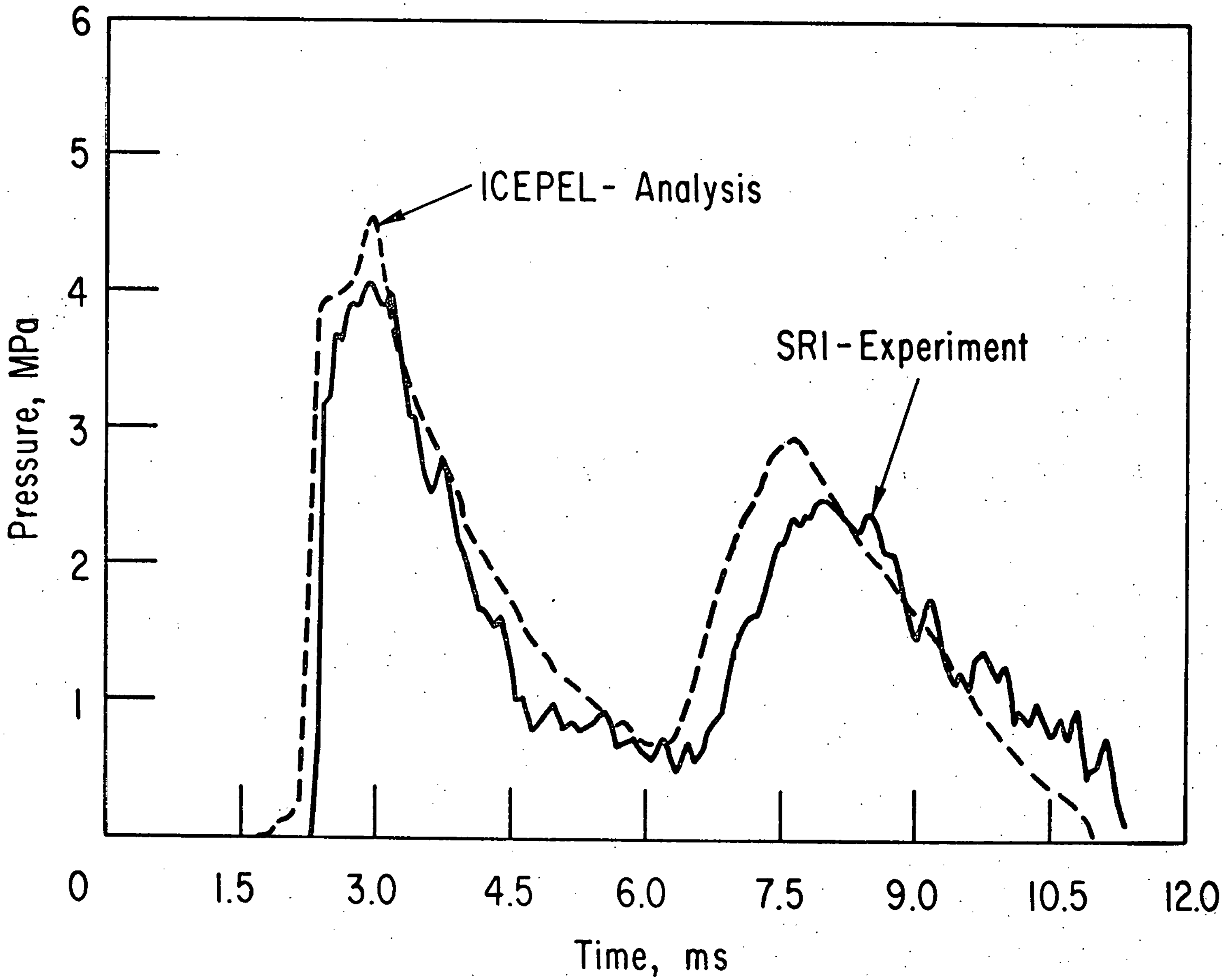

Fig. 9. Analytical and Experimental Pressure Histories at Location P7 of the First Flexible Pipe.

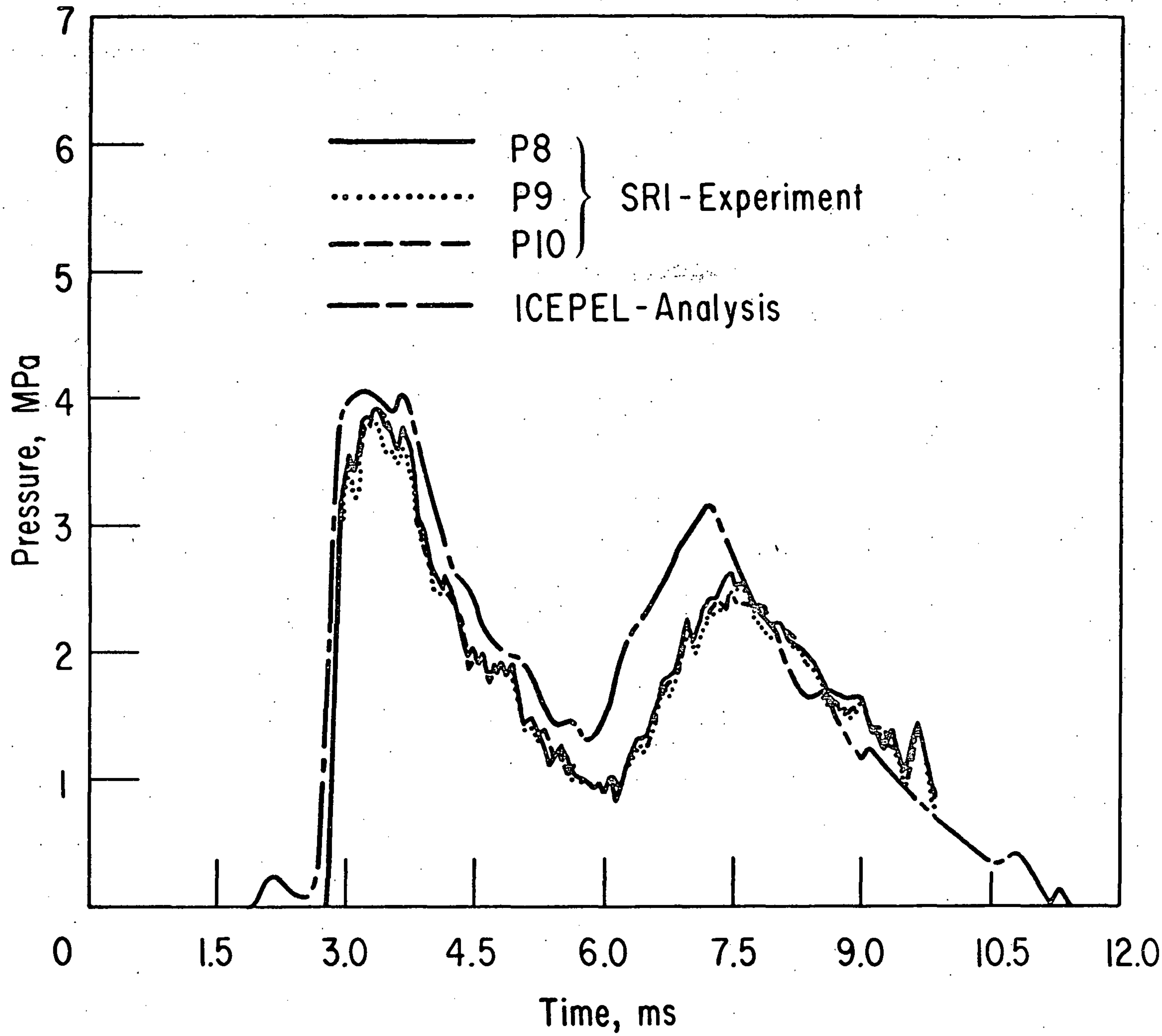

Fig. 10. Analytical and Experimental Pressure Histories at Locations P8–P10 of the First Flexible Pipe.

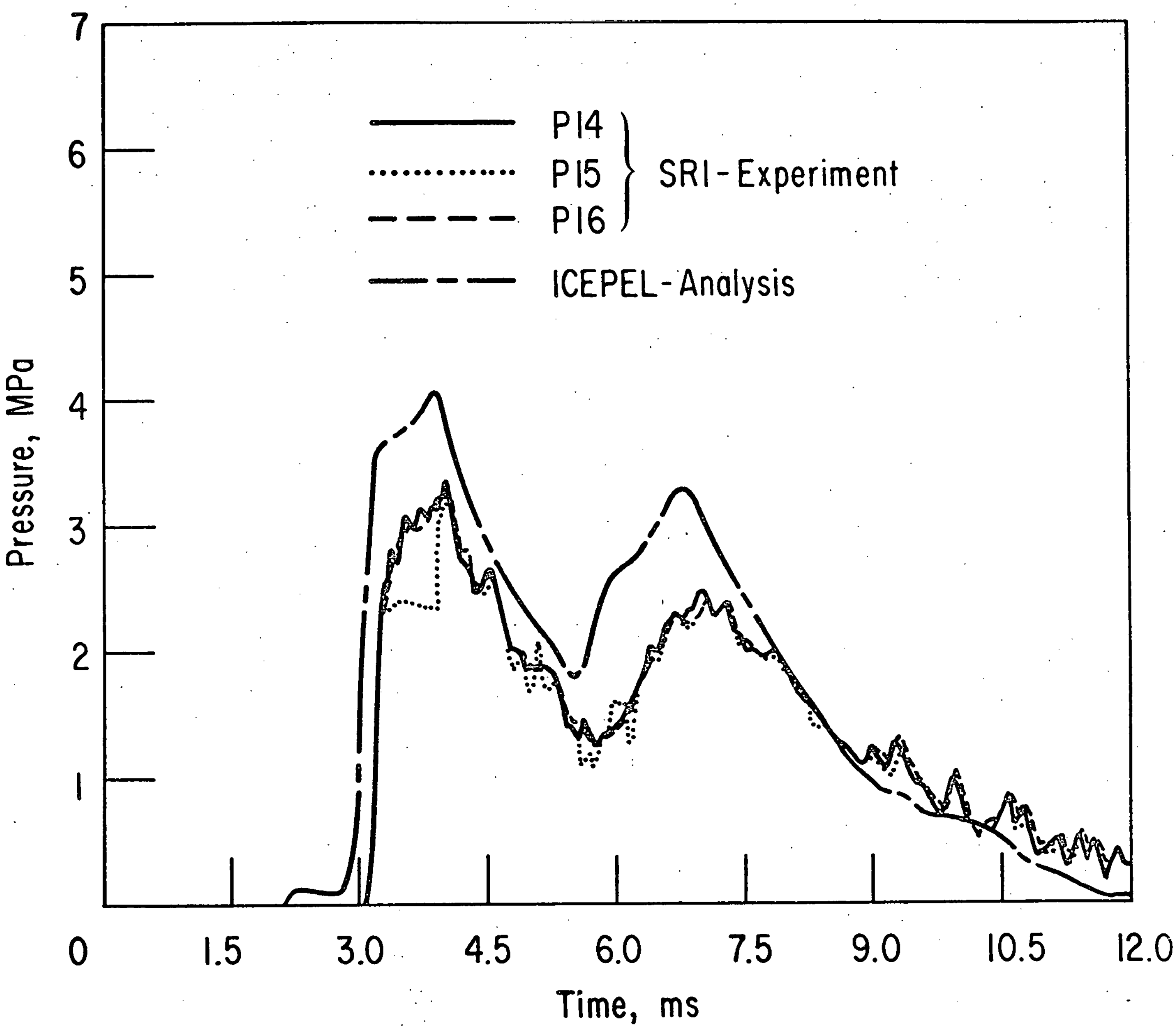

Fig. 11. Analytical and Experimental Pressure Histories at Locations P14–P16 of the Second Flexible Pipe.

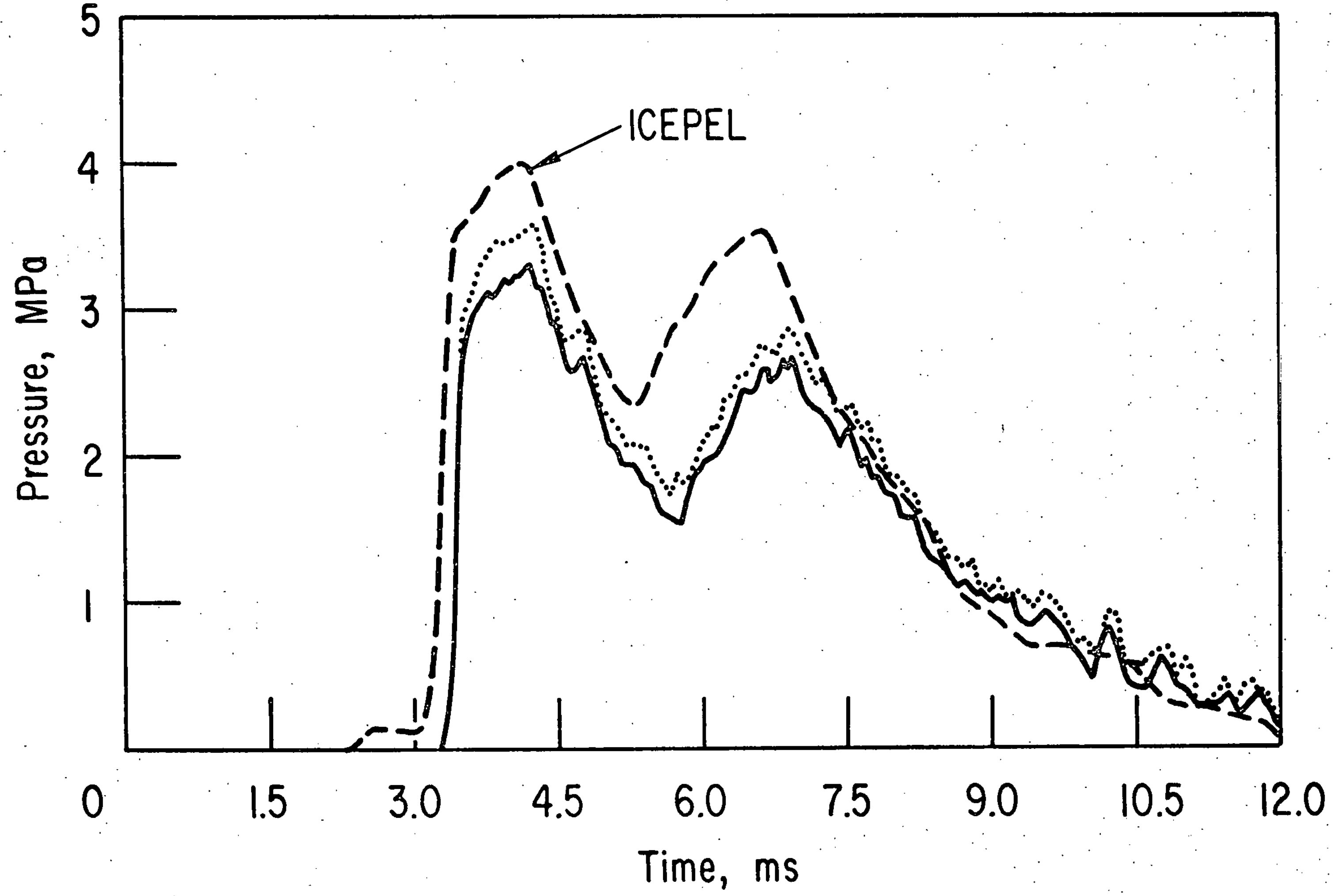

Fig. 12. Analytical and Experimental Pressure Histories at Locations P17 and P18 of the Second Flexible Pipe.

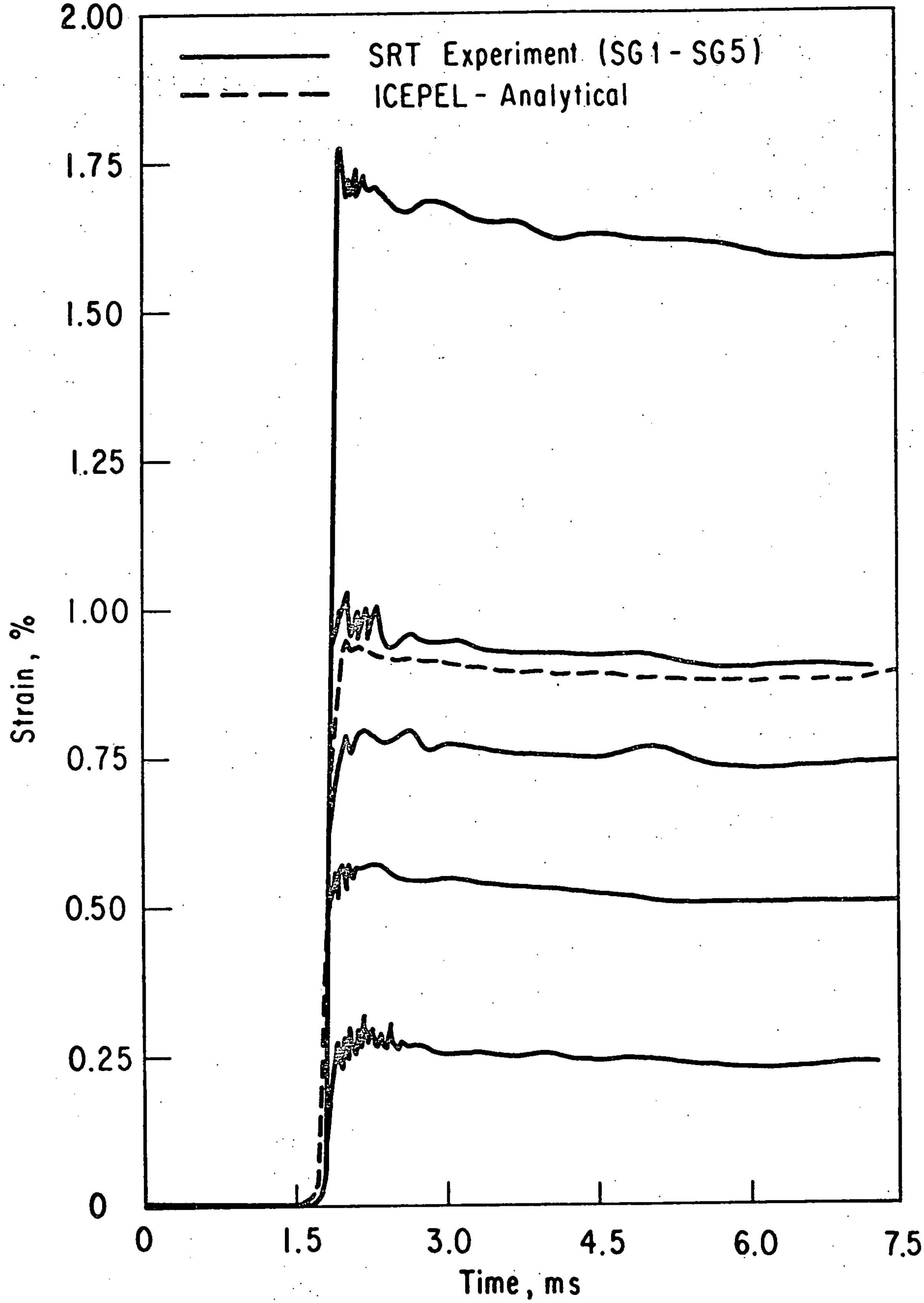

Fig. 13. Analytical and Experimental Circumferential Strain Histories at 3.81 cm into the First Flexible Pipe.

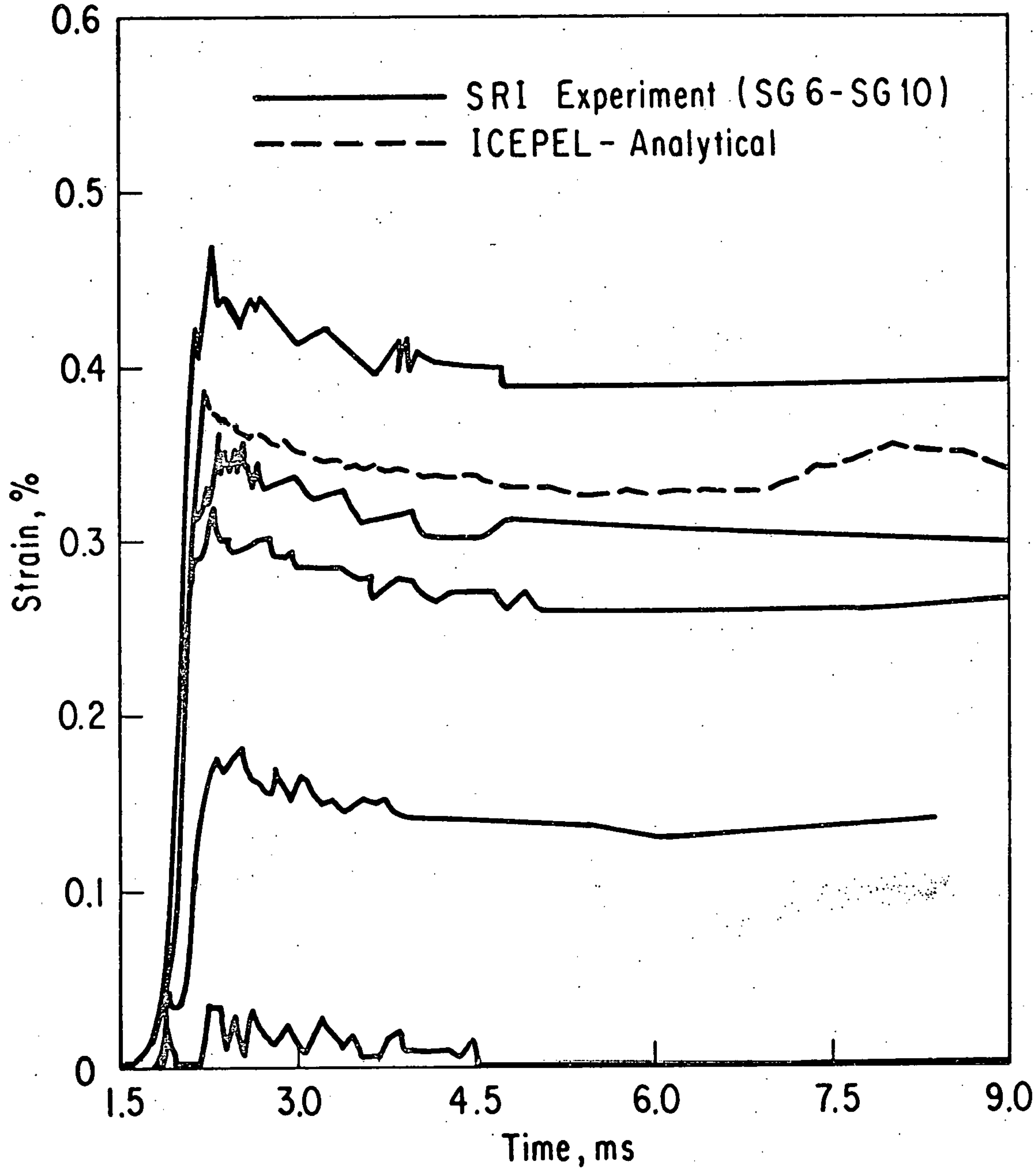

Fig. 14. Analytical and Experimental Circumferential Strain Histories at 15.74 cm into the First Flexible Pipe.

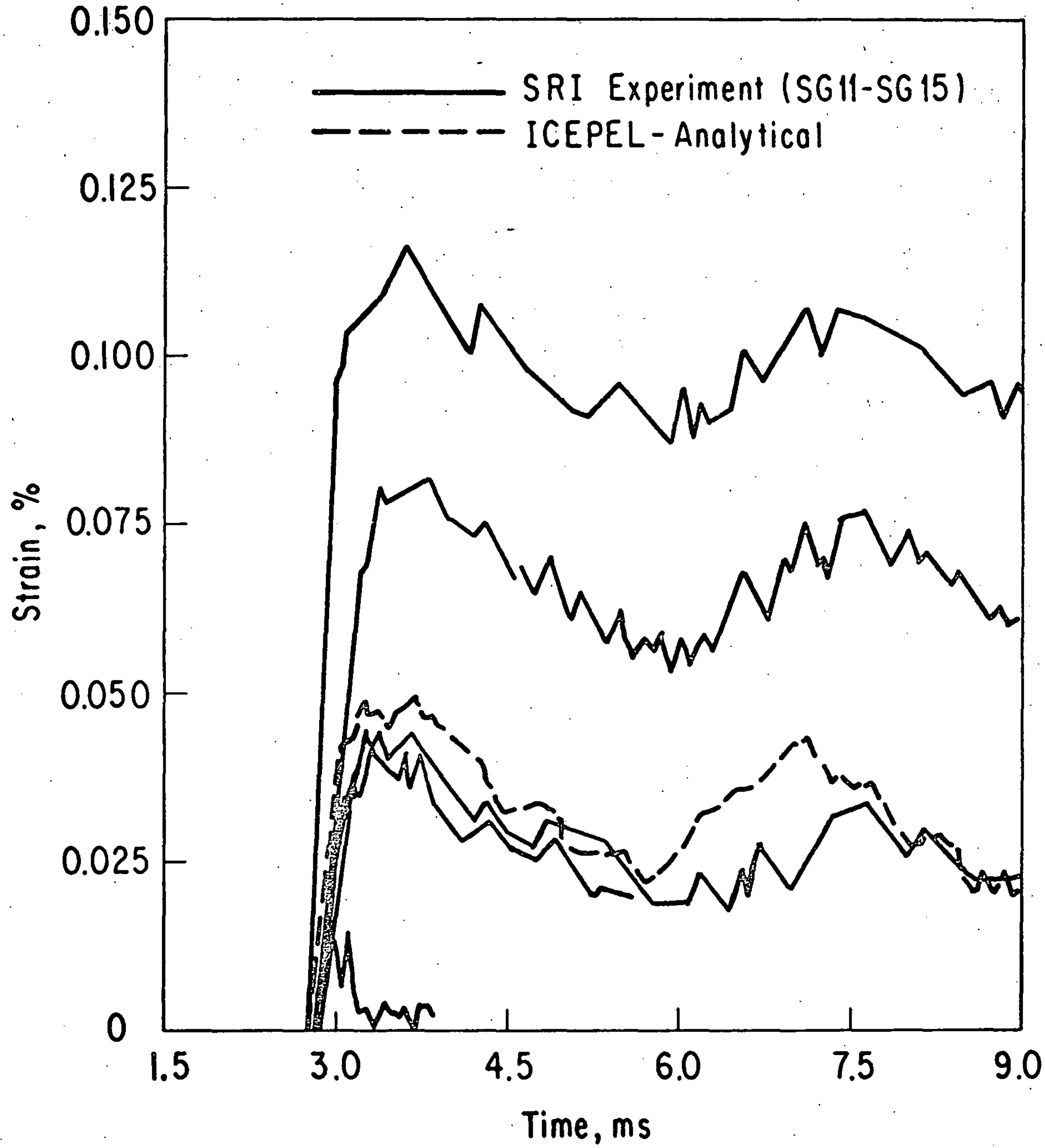

Fig. 15. Analytical and Experimental Circumferential Strain Histories at 15.24 cm from the Elbow in the First Flexible Pipe.

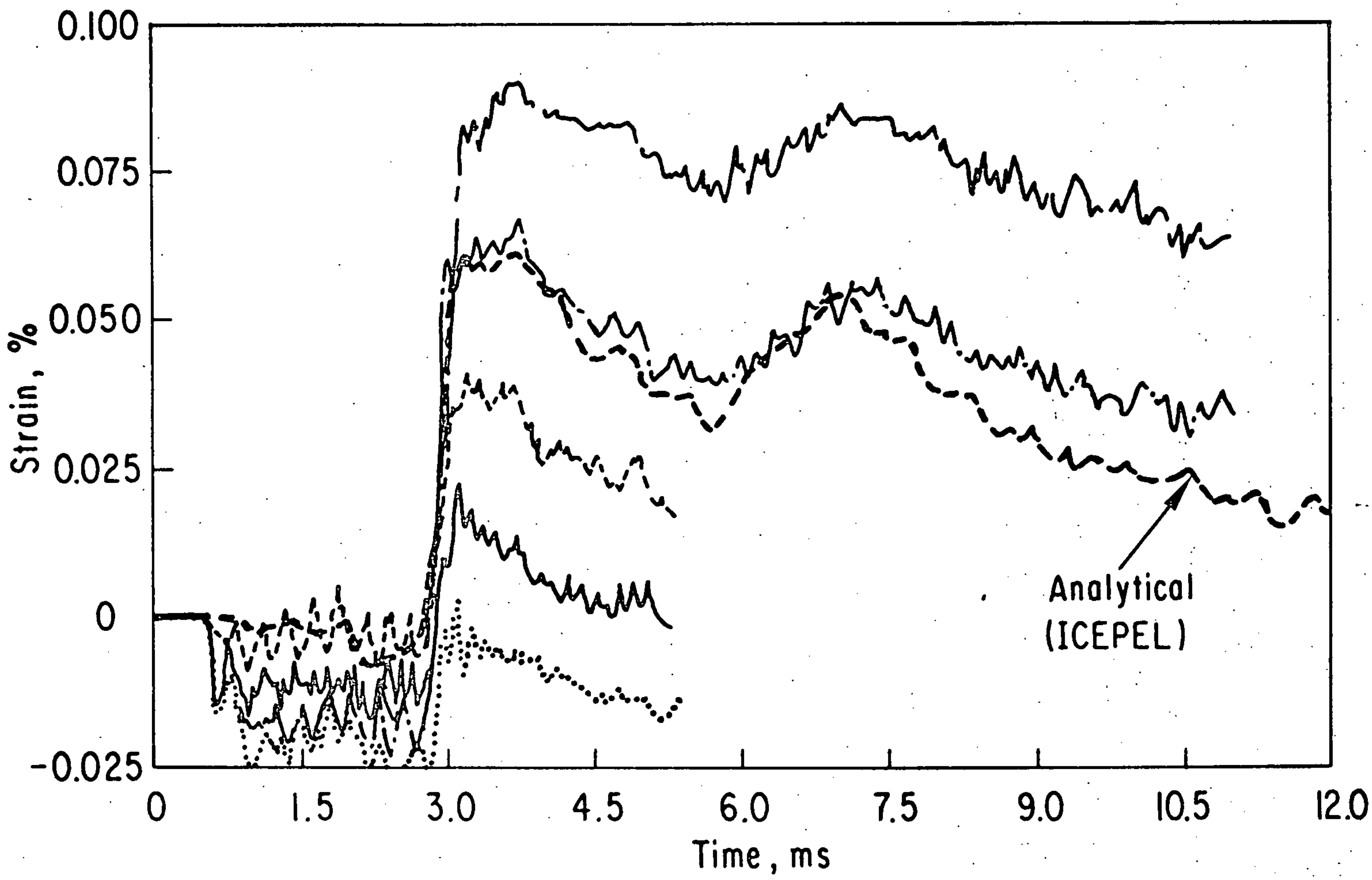

Fig. 16. Analytical and Experimental Circumferential Strain Histories at 3.81 cm from the Elbow in the First Flexible Pipe.